Study of the Guided Wave Sensing by Hybrid Piezoelectric-FBG Approach

SULTAN AHAMAD, PAWEL H. MALINOWSKI,
ROHAN SOMAN and TOMASZ WANDOWSKI

ABSTRACT

In this research, analysis of ultrasonic guided wave sensing using fiber optic strain sensors based on fiber Bragg gratings (FBG) is presented. Wave excitation is based on piezoelectric transducers. Sensitivity of the FBG sensors to propagating ultrasonic waves plays an important role in the design process of SHM system based on fiber optic sensors. The presented study has experimental character. Separation of symmetric and antisymmetric modes is studied based on simultaneous sensing of the guided waves with two FBG sensors. The influence of actuation is studied for various frequencies of excitation. Moreover, influence of piezoelectric transducers with different diameters on the wave signals registered at the FBG sensors is investigated. The obtained results show significant impact of the diameter of the piezoelectric actuators on the guided waves signals registered by FBGs.

INTRODUCTION

Structural health monitoring (SHM) helps in reducing maintenance costs and avoiding several types of structural failures. It is necessary to carry out health monitoring and evaluation of engineering structures to put an end to the potential hazards and improve the safety performance of structures. A number of defects generally occur in the structures, like cracks, corrosion, etc. There are some parameters that are generally used for SHM, like vibration, electromechanical impedance, strain, etc. In order to assess the structural health of a system, it is necessary to identify characteristics based on collected data that make it possible to differentiate between the undamaged (referential or pristine) and damaged structure [1]. SHM processes for structures are generally based on the comparison of healthy and unknown (damaged) databases. One of the various diagnostic techniques available in SHM is the guided wave (GW) propagation approach [2].

Sultan Ahamad, Paweł H. Malinowski, Rohan Soman, Tomasz Wandowski, Institute of Fluid Flow Machinery, Polish Academy of Sciences, 80-231 Gdańsk, Poland

The guided waves are generally excited (actuated) using the piezoelectric transducer (PZT), and sometimes there are more than one PZT as actuators at different positions for helping in the damage localization process. PZT transducers can be used for elastic wave excitation in a broad frequency spectrum. This property made them particularly suitable for the SHM [3]. Elastic waves can interact with structural discontinuities caused by various types of damage, making PZT use for structural health monitoring successful [4]. A PZT transducer can act as both an actuator and a sensor. The PZT sensor is inexpensive but requires a sensing connection with metallic wires, so it has drawbacks such as EMF (electromotive force) generation caused by flowing current, high noise, and weight. To deal with these issues, a large number of recent research used the Fiber Bragg Grating (FBG) sensor, which avoids concerns such as EMF, high noise generation, and weight because that is based on an optical fiber. FBG has been employed for SHM research studies at a very large scale in recent years [5]. FBG works as a sensor. There are a large number of research studies employing it in different configurations and also some other sensors. It is a great contribution to SHM by research on the sensing part, but actuation also plays a key role in guided wave-based SHM. Freitas et al. presented an experimental analysis of the feasibility of low-cost piezoelectric diaphragms in impedance-based SHM applications [6]. They evaluated the diaphragms of different sizes in aluminum beams and compared the experimental results with those obtained from a conventional PZT ceramic.

Aabid et al. presented a review of piezoelectric actuator applications in damaged structures [7]. They reviewed the use of PZT actuators in damaged structures and adhesively bonded combined systems using three different repair investigation methods: analytical, numerical, and experimental.

Jin et al. recently presented a review on PZT actuators based on high-performance piezoelectric materials [8]. Similarly, few relevant studies are available, but no serious and directly related study is available which makes the comparison of different PZTs for SHM application. More and more research studies are needed presenting the comparison of different PZTs as the actuator. Additionally, due to the reason that the sensing part is getting popular using FBG, the sensing should be performed using FBG sensors, preferably by using FBGs in different styles/configurations.

This paper compares the results for the actuation of three different diameters of PZTs for SHM applications. The two FBGs were placed, one at the top and another at the bottom sides of an aluminum plate, for sensing from both sides of the sample. Because of the longitudinal/transverse nature of these waves, this dual-side simultaneous sensing has been performed to make the possibility of S0, A0 Mode separation.

This paper presented the amplitude comparison of signals generated by all three PZTs. It demonstrates the comparison of signals simultaneously sensed by top and bottom FBGs. Furthermore, this paper presented analysis for frequencies in the 60-250 kHz range analysis and comparison by presenting the time vs. (normalized) amplitude graphs. These graphs were compared with numerically calculated dispersion curves. The paper also presents the addition and subtraction of top and bottom FBGs' signals to investigate them in a more advanced manner.

EXPERIMENT DESCRIPTION

Figure 1 shows the schematic sketch of the experimental setup. The sample used is an aluminum plate of size 1 m x 1 m x 0.001 m. In the center of the plate, the PZT actuator is bonded. In this research, different diameters of PZTs were investigated. At a distance of 0.25 m from the center, two FBGs are attached to the plate, one at the top side (FBG_T) and another at the bottom side (FBG_B). The FBGs manufactured by Femto Fibertech were used. A tunable Laser source (Apex AP1000) has been used. The oscilloscope used here is of National Instruments PXIe-5105 PXI, and the amplifier is Krohn Hite 7500. The actuation of the waves was made by excitation of the five-cycle Hann windowed signal at different frequencies (60–250 kHz at a step of 10 kHz) using the arbitrary waveform generator. Then it was amplified in a voltage amplifier, and finally, it actuated the PZT, which generates the guided waves in the plate. Three PZTs of 10, 20, and 30 mm diameter were used (0.5 mm thickness). First, the frequencies of 60-250 kHz were generated through 10 mm PZT. After that, the 10 mm PZT was removed, and at the same place, the PZT of 20 mm was used for the same task. The same procedure was followed for the 30 mm PZT. As shown in Figure 1, the sensing was made by two FBGs attached to the aluminum plate. Both sensors recorded the wave signals on both sides of the plate. The initial comparison focused on single signals for three sizes of the actuating transducer and for an arbitrarily chosen frequency (120 kHz). The signals are shown in Figure 2. The signals are not identical. The differences in amplitudes are visible as well as additional wave packets appear for 20 and 30 mm transducers.

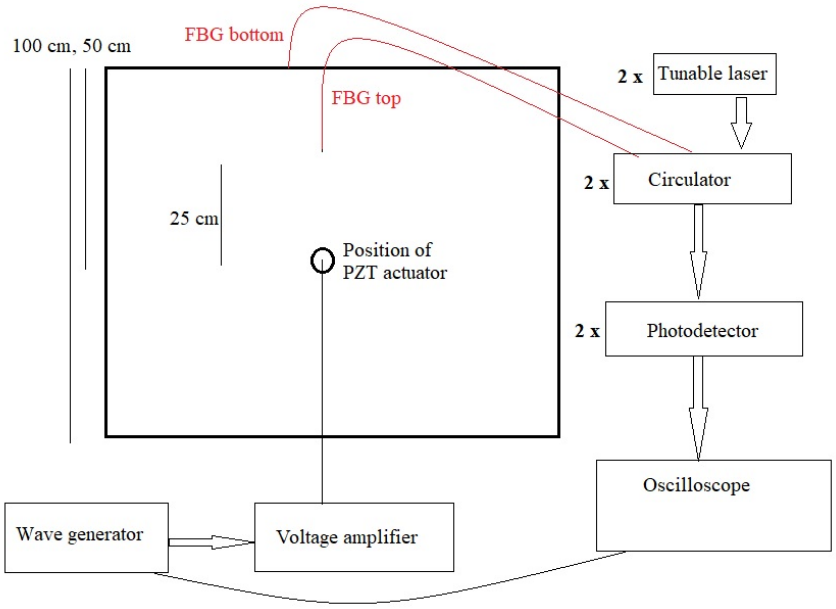

Figure 1. The schematic diagram of the experimental setup.

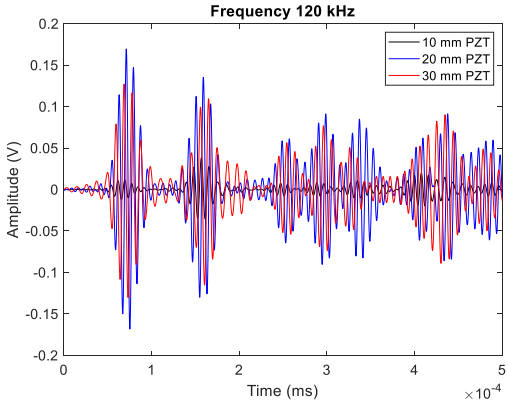

Figure 2. Comparison of actuation by three different size PZTs, the signals were sensed by FBG_T.

There are also differences if one looks at the comparison of top and bottom FBG signals response for the same size of the actuating transducer (Figure 3). In the case of 10 mm transducers the difference is most pronounced at latter part of the signal, but for the remaining two the significant difference is visible near the second wave packet.

METHOD OF COMPARISON

In order to compare the registered signals the envelope (Hilbert transform used) was applied on both top and bottom FBG signals separately, and both signals were normalized. The amplitude normalized times signals of both top and bottom FBGs were plotted for a 60-250 kHz frequency range in a surface plot. On the same plots, numerically calculated dispersion curve values were taken from the Vallen system (dispersion) software [9]. The curve was in the frequency and velocity domain. Our experiment is based on a 25 cm distance between the sensor and the actuator. So using the numerically calculated values of Vallen software, we calculated the time taken by waves for each frequency to reach the 25 cm distance. In this experiment, the distance to the closest edge is 50 cm. The distance between the actuator and the sensor is 25 cm. So the first wave reflection reaching the sensor will be from (50+25 cm) 75 cm. So based on the velocities, we also calculated the time taken by waves to reach 75 cm, and thus the first reflections of S0 and A0 both were also indicated in the graphs. Thus our graph includes the theoretical time of arrival of direct waves and the first reflection from 75 cm.

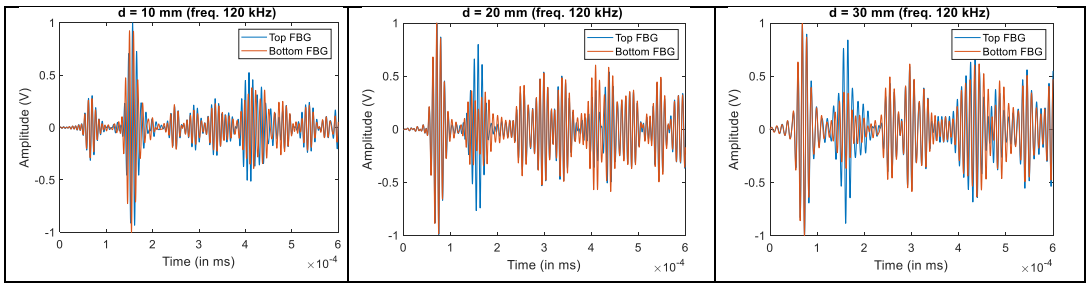

Figure 3. Comparison of sensing by top and bottom FBG sensors for each size of the actuating transducer.

Numerically calculated lines were plotted using red color for S0 and using blue color for A0. The reflections of waves of S0 and A0 were plotted by the same colors as their direct waves, i.e., S0 (red) and A0 (blue). The reflection comes after sometimes of the direct wave. Also, the addition and subtraction of signals was applied. It should be helpful because of the nature of symmetric and antisymmetric waves (in-phase/out-phase). For examining the addition of top and bottom FBG signals, the envelope was applied to the signals of top and bottom FBGs. Then these signals were normalized and then added. After addition, these were again normalized for visualization. Then, these additions were plotted In the same manner the subtraction was performed.

RESULTS

The frequency by frequency comparison is not too much effective and bit problematic, so the method described in the previous section was applied. Figures 4, 6 and 8 present results for all three PZTs. The solid color lines represent the theoretical time of arrival and are ordered from the left-hand side as follows: first red – S0, second red – reflections of S0, first blue- A0, second blue- reflection of A0. The first arrivals of S0 mode for all the sizes of transducers were predicted with good accuracy. The influence of the transducer size is visible for the lower frequencies, especially for 10 mm transducer, for which there was not effective excitation of the S0 mode. On the other hand the A0 was excited for this lower frequency range. The direct arrival of A0 mode is close in time to the edge reflected S0 so they are overlapping and the separation for some frequencies in not obvious. In order to enhance the visualization of single modes subtraction and addition was performed and shown in Figures 5, 7 and 9. The direct arrival of the S0 was effectively removed by the subtraction. But the removal of the A0 was not so effective, probably due to overlap with edge reflected S0.

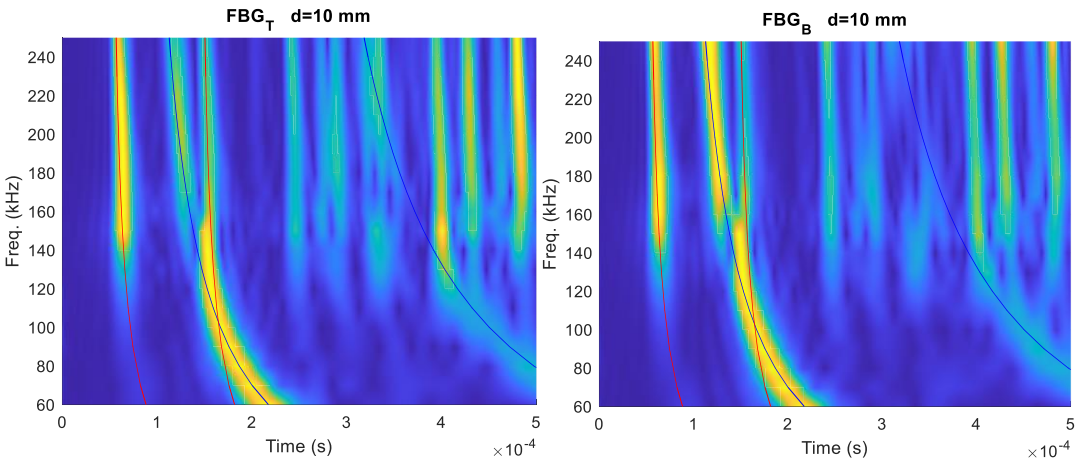

Figure 4. Registered time signals for top (FBG_T) and bottom (FBG_T) sensors for actuation at 10 mm transducer; solid lines represent the theoretically predicted arrival of direct and edge reflected S0 and A0 modes.

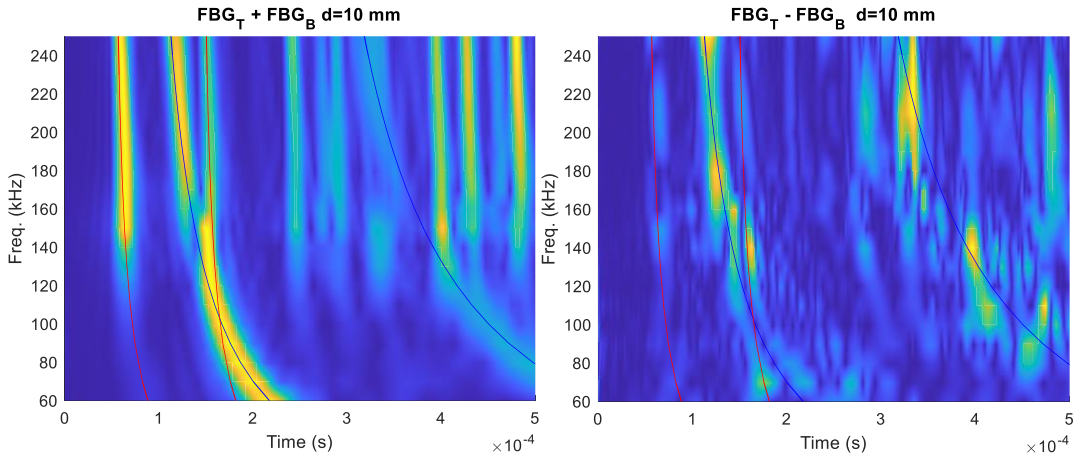

Figure 5. Time signals addition and subtraction for actuation at 10 mm transducer; solid lines represent the theoretically predicted arrival of direct and edge reflected S0 and A0 modes.

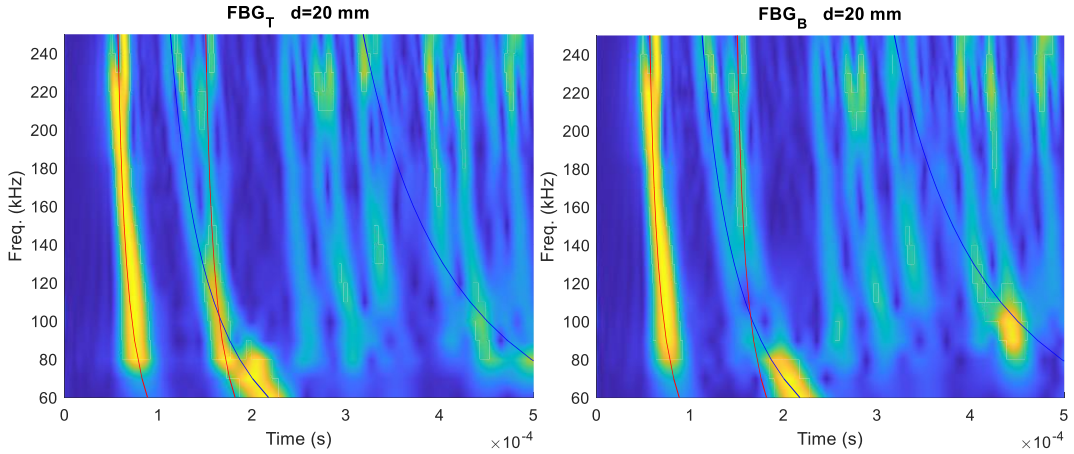

Figure 6. Registered time signals for top (FBG_T) and bottom (FBG_T) sensors for actuation at 20 mm transducer; solid lines represent the theoretically predicted arrival of direct and edge reflected S0 and A0 modes.

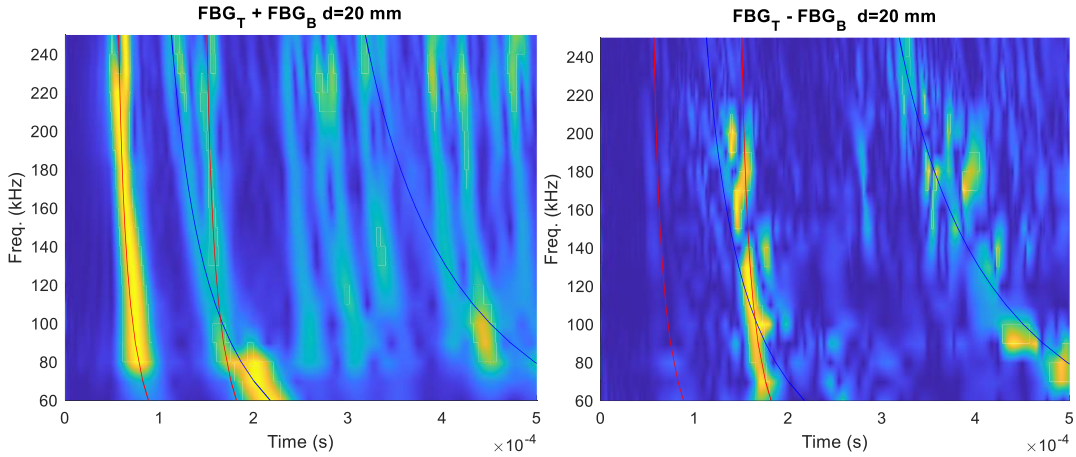

Figure 7. Time signals addition and subtraction for actuation at 20 mm transducer; solid lines represent the theoretically predicted arrival of direct and edge reflected S0 and A0 modes.

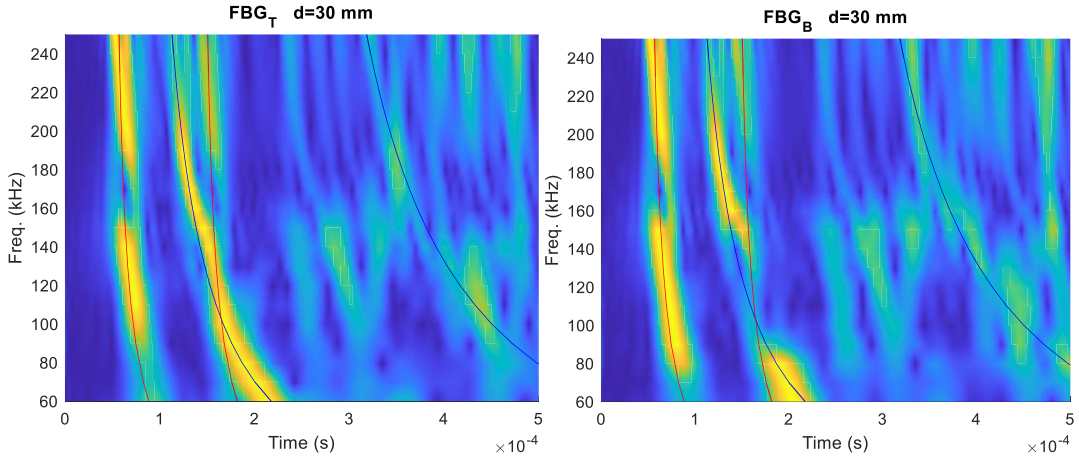

Figure 8. Registered time signals for top (FBG_T) and bottom (FBG_T) sensors for actuation at 30 mm transducer; solid lines represent the theoretically predicted arrival of direct and edge reflected S0 and A0 modes.

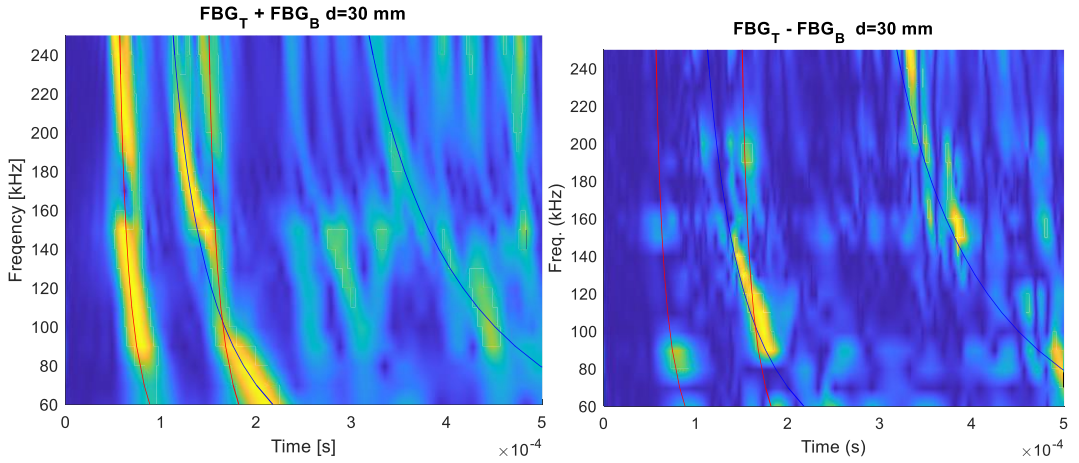

Figure 9. Time signals addition and subtraction for actuation at 30 mm transducer; solid lines represent the theoretically predicted arrival of direct and edge reflected S0 and A0 modes

DISCUSSION AND CONCLUSIONS

The paper presented a comparison of different size PZTs as the actuators and sensing by dual FBG set up. The significant difference in the actuation of signals by different sizes PZTs at the same frequency is visible. A good match of the experimental data with the theoretically predicted wave arrivals was obtained. By applying the addition and subtraction of the registered data, it was possible to reduce the influence of respective modes. It was shown that for frequencies near 100 kHz, there is a problem of separation of the A0 and S0 mode due to the overlap of the direct A0 wave with the edge-reflected S0 wave. It is foreseen that this research will be useful for many research studies in SHM employing different sizes of PZT and FBG-based dual-side sensing.

ACKNOWLEDGMENTS

The authors would like to gratefully acknowledge the support given by the National Science Centre, Poland under grant agreement no. 2020/39/B/ST8/01753 in the frame of the OPUS project entitled: " Study of elastic wave mode sensing and separation using FBG sensors for structural health monitoring". The authors also acknowledge Task-CI for allowing use of computational resources.

REFERENCES

1. Bayoumi, A., Minten, T. & Mueller, I. 2021. "Determination of Detection Probability and Localization Accuracy for a Guided Wave-Based Structural Health Monitoring System on a Composite Structure" *Applied Mechanics* **2**, 996–1008.
2. Mitra, M. & Gopalakrishnan. 2016. "S. Guided wave based structural health monitoring: A review" *Smart Mater Struct* **25**, 053001.
3. Dziendzikowski, M., Heesch, M., Gorski, J., Dragan, K. & Dworakowski, Z. 2021. "Application of pzt ceramic sensors for composite structure monitoring using harmonic excitation signals and bayesian classification approach" *Materials* **14**.
4. Sevillano, E., Sun, R. & Perera, R. 2016."Damage Detection Based on Power Dissipation Measured with PZT Sensors through the Combination of Electro-Mechanical Impedances and Guided Waves" *Sensors 2016, Vol. 16, Page 639* **16**, 639.
5. Dutta, C., Kumar, J., Das, T. K. & Sagar, S. P. 2021. "Recent Advancements in the Development of Sensors for the Structural Health Monitoring (SHM) at High-Temperature Environment: A Review" *IEEE Sens J* **21**, 15904–15916.
6. Silva De Freitas, E. & Guimarães Baptista, F. 2016. "Experimental analysis of the feasibility of low-cost piezoelectric diaphragms in impedance-based SHM applications" *Sens Actuators A Phys* **238**, 220–228.
7. Aabid, A., Hrairi, M., Mohamed Ali, S. J. & Ibrahim, Y. E. 2022. "Review of Piezoelectric Actuator Applications in Damaged Structures: Challenges and Opportunities" *ACS Omega* doi:10.1021/ACSOMEGA.2C06573/ASSET/IMAGES/LARGE/AO2C06573_0012.JPEG.
8. Jin, H. *et al.* 2022. "Review on Piezoelectric Actuators Based on High-Performance Piezoelectric Materials. *IEEE Trans Ultrason Ferroelectr Freq Control* **69**, 3057–3069.
9. Vallen Systeme GmbH - EC TEST Systems. https://www.ects.pl/produkty/producenci/vallen-systeme/.